Applying CFD in the Analysis of Heavy-Oil Transportation in Curved Pipes Using Core-Flow Technique

S Conceição[1], A Lima[1]*, T Andrade[1], S Neto[1], V Oliveira[2], K Angelim[1], L Rocha[1]

1. Federal University of Campina Grande, Brazil.
2.State University of Paraíba, Brazil

ABSTRACT

Multiphase flow of oil, gas and water occurs in the petroleum industry from the reservoir to the processing units. The occurrence of heavy oils in the world is increasing significantly and points to the need for greater investment in the reservoirs exploitation and, consequently, to the development of new technologies for the production and transport of this oil. Therefore, it is interesting improve techniques to ensure an increase in energy efficiency in the transport of this oil. The core-flow technique is one of the most advantageous methods of lifting and transporting of oil. The core-flow technique does not alter the oil viscosity, but change the flow pattern and thus, reducing friction during heavy oil transportation. This flow pattern is characterized by a fine water pellicle that is formed close to the inner wall of the pipe, aging as lubricant of the oil flowing in the core of the pipe. In this sense, the objective of this paper is to study the isothermal flow of heavy oil in curved pipelines, employing the core-flow technique. A three-dimensional, transient and isothermal mathematical model that considers the mixture and k-ε turbulence models to address the gas-water-heavy oil three-phase flow in the pipe was applied for analysis. Simulations with different flow patterns of the involved phases (oil-gas-water) have been done, in order to optimize the transport of heavy oils. Results of pressure and volumetric fraction distribution of the involved phases are presented and analyzed. It was verified that the oil core lubricated by a fine water layer flowing in the pipe considerably decreases pressure drop.

1. INTRODUCTION

The multiphase flow of oil, gas and water occurs in the oil industry from the reservoir to the processing units. The Brazilian scenario shows that as light oil reserves are scarce, the production of heavy hydrocarbons is the only possible alternative future. In this way, we are looking for technologies that will minimize possible problems due to the production of heavy oil.

Problems related to the fluid flow in pipes are easily found in engineering practice. Situations that seek information fluids flow through tubes, calculation of energy conversions, influences of variables such as viscosity, density and roughness are commonly found.

*Corresponding Author: antonio.gilson@ufcg.edu.br

As regards to the transport of this type of hydrocarbon, it can be stated that as high viscosity

and density and a high pressure drop by friction that occurs during the flow are common situations. These conditions require an excessive workload of the equipment and hence a high energy demand, which becomes economically unviable the production of these oils.

Due to its unfavorable characteristics, transportation from the production areas to the processing and refining plants is the greatest difficulty encountered in the production of heavy oils. The most commonly used alternatives are trucking or heated piping. However, these methods are costly and apply only for short distances [1]. Among the main techniques applicable to deepwater production are temperature control, flow control and dilution with light oil [2].

All possible ways of solving the problem of heavy oil transportation is related to the same principle, which is to control its physicochemical properties. Some other methods are also used, both for offshore and onshore fields: heating the oil with the injection of a heated fluid, or through electric heating; Generation of oil emulsions in water; Injection of water in pipe to form an "insulating" film (ring) that surrounds the oil (core-flow).

The core-flow technique consists of injecting water into the sides of the pipeline, at lower flow rates than the oil, in order to obtain an annular flow pattern, where the water flows as a continuous phase forming a film that surrounds the oil, avoiding contact of the oil with the duct walls consequently reducing the pressure drop by friction. Them, developing alternatives to ensure not only the efficiency of transport but also energy efficiency is currently one of the great challenges of the oil industry.

In view of the above this study aims to numerically study the three-phase flow, isothermal, and three-dimensional and transient flow in curved pipes via CFD. Highlight are related to multiphase modeling; evaluate the effect of the volumetric fraction on the hydrodynamic of the flow; to find an operating range in which the reduction of the pressure drop associated to a reduction of energy consumption is guaranteed; and finally evaluate the influence of temperature on water pumping.

2. HEAVY-OIL TRANSPORT TECHNIQUES

The main objective of the core-flow technique, according to Trevisan [1], is to obtain a considerable reduction in the pressure drop along the flow, since the viscosity of the heavy oil is the main disadvantage. In this way its influence is minimized, since the water acts as a lubricant. Figure 1 illustrates a duct in which it is possible to visualize the use of core-flow technique.

The core-flow study began decades ago where it was first cited by Russel et al. [3] referenced by Obregón [4]. This method was devised by Isaacs and Speed in 1904, referred to U.S. Patent No. 759374, mentioning the ability to transport viscous products by means of water lubrication. It was subsequently tested in an experimental manner generating results that already pointed to a reduction of pressure loss in the flow line.

Several authors have studied heavy-oil transportation using the core-flow technique. From these works, in some studies have been carried out on the behavior of the annular flow pattern for water-oil two-phase flow [5,6]. The presence of the gas during an oil production is constant. The gas, which was initially in solution without oil, is released forming different media during the flow. These patterns were identified experimentally as reported by Trevisan [1], Wegmann et al. [7] and Poesio et al. [8]. However, the influence of the gas phase in the

core-flow on pipelines and connections is still not well defined, and further studies are needed to ensure the efficiency of the technique in this physical situation. The tests of the related phenomena that emerged in connections were evaluated by Wang et al. [9], Andrade et al. [10], Andrade et al. [11], Andrade et al. [12], Andrade et al. [13] and Crivelaro et al. [14].

Figure 1. Schema of the two-phase (oil and water) flow via core-flow

Particularly with reference to reduction of pressure drop in flow, Brauner et al. [15] has reported a correlation applied to heavy-oil/water two-phase flow in an annular flow pattern. Vanegas [16] verified a reduction in pressure drop up to 93 times as compared to the single-phase oil flow, thus, a correlation was developed to predict the pressure drop in the flows. Similar results was reported by Bannwart [17].

3. METHODOLOGY

3.1 The geometry and numerical mesh

The geometric domain was determined by the definition of points, curves, surfaces and solids describing the desired size and shape. In this way the duct under study was created computationally with a radius 15 cm, containing 3 m length before the curvature along the z axis, and 3 m after the curvature along the axis and. The curvature has a radius 20 cm with an angle 90 °. Figure 2 shows an overview of the geometry used.

From the geometry was possible to develop the structured computational mesh composed by 289552 hexahedral elements in the ANSYS ICEM CFD® module. Due to the complexity of the problem some regions, such as curvature, for example, needed further refinement, in order to obtain results that are closer and consistent with physical reality. Figure 3 illustrates the inlet and outlet regions of the mesh used.

3.2 Multiphase mathematical modeling

3.2.1 Governing equations

The mathematical conditions assumed refer to an Eulerian-Eulerian study with an inhomogeneous approach. These considerations make possible a study in which each phase has its flow field; thus, we have a set of solutions for each phase separately. The phases present in the flow are represented by the letters α, β, and γ.

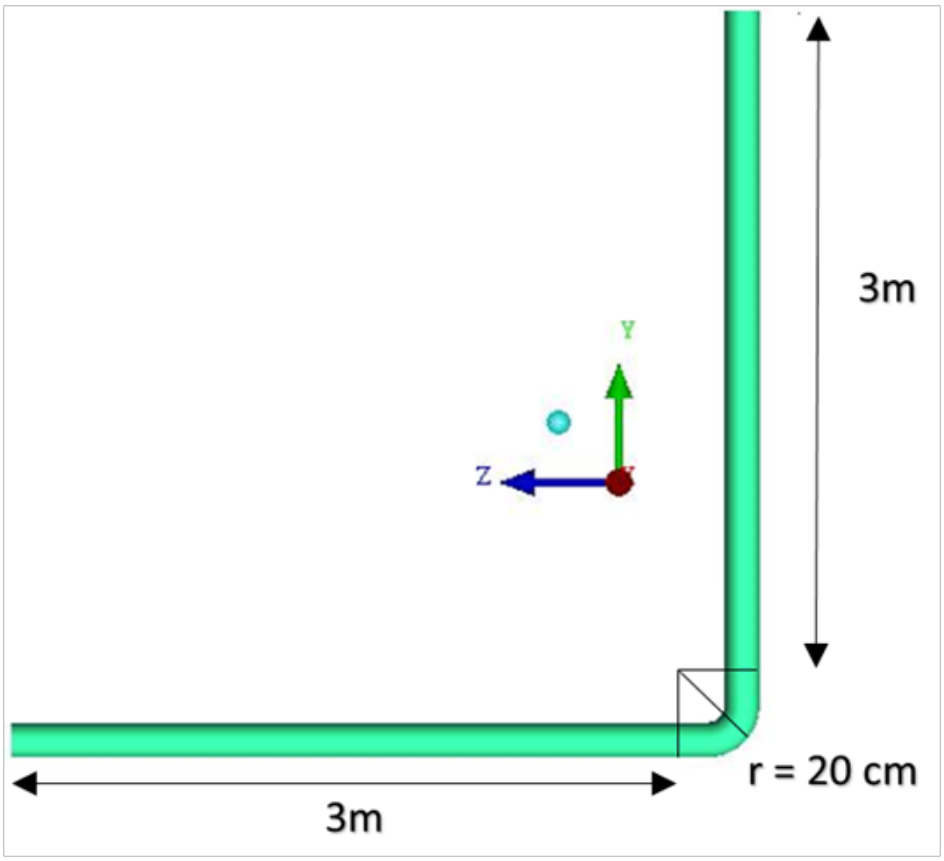

Figure 2. Geometry of the duct with 6 m length and 15 cm diameter

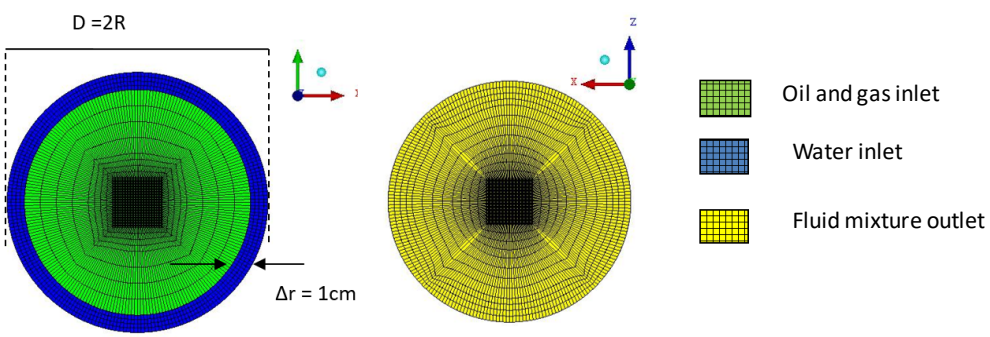

Figure 3. Numerical mesh with detail on the input and output region

The general conditions for the three-phase flow (water-oil-gas) were: isothermal and non-isothermal, transient, three-dimensional, and incompressible flow, considering constant thermo-physical properties, no mass transfer and presence of body force. To model the three-dimensional multiphase flow, the following equations were used:

- Mass Conservation Equation:

$$\frac{\partial}{\partial t}\left(f_\alpha \rho_\alpha\right) + \nabla \cdot \left(r_\alpha \rho_\alpha \vec{U}_\alpha\right) = 0 \tag{1}$$

- Momentum Conservation Equation:

$$\frac{\partial}{\partial t}\left(f_\alpha \rho_\alpha \vec{U}_\alpha\right) + \nabla \cdot \left[f_\alpha (\rho_\alpha \otimes \vec{U}_\alpha)\right] - f_\alpha \nabla p_\alpha + \nabla \cdot \left\{f_\alpha \mu_\alpha \left[\nabla \vec{U}_\alpha + (\nabla \vec{U}_\alpha)^{.T}\right]\right\} = \vec{S}_{M\alpha} + \vec{M}_\alpha \tag{2}$$

where is assumed that for the α phase, f is the volume fraction, ρ is the density, $\vec{U}$ is the velocity vector, μ is the dynamic viscosity, p is the pressure, the term $\overrightarrow{S_{M\alpha}}$ describes the linear moment due to external body strength (gravitational force), while $\vec{M}_\alpha$ describes the interfacial forces (drag force, lift force, virtual mass force, wall lubrication force and turbulent dispersion force at the interface), these forces act on the phase α due to the presence of other phases.

- Energy Conservation Equation:

$$\frac{\partial}{\partial t}\left(f_\alpha \rho_\alpha h_\alpha\right) + \nabla \cdot \left[f_\alpha \left(\rho_\alpha \vec{U}_\alpha h_\alpha - \lambda_\alpha T_\alpha\right)\right] = \sum_{\beta=1}^{N_p} \left(\Gamma^+_{\alpha\beta} h_\beta - \Gamma^+_{\alpha\beta} h_\alpha\right) + Q_\alpha + S_\alpha \tag{3}$$

where $\rho_\alpha, h_\alpha, \lambda_\alpha$ and T_α represent the density, static enthalpy, thermal conductivity and temperature of phase α, respectively; S_α is the external heat source; Q_α represents the heat transfer to the α phase through the interfaces with other phases, and the term $(\Gamma^+_{\alpha\beta} h_\beta - \Gamma^+_{\alpha\beta} h_\alpha)$ represents heat transfer induced for mass transfer. The heat transfer at the interface occurs due to thermal non-equilibrium through the interface of the phases.

The total heat per unit volume transferred to the phase α due to the interaction with other phases and denoted Q_α is given by:

$$Q_\alpha = \sum_{\alpha \neq \beta} Q_{\alpha\beta} \tag{4}$$

or yet

$$Q_{\alpha\beta} = Q_{\beta\alpha} = \sum_{\alpha} Q_\alpha = 0 \tag{5}$$

The heat transfer rate $Q_{\alpha\beta}$ per unit time, through the interfacial area density, per unit volume $A_{\alpha\beta}$ from the phase α to the phase β is given by:

$$Q_{\alpha\beta} = h_{\alpha\beta} A_{\alpha\beta}(T_\alpha - T_\beta) \tag{6}$$

Equation (6) can also be written as follows:

$$Q_{\alpha\beta} = C_{\propto\beta}^{(h)} (T_\alpha - T_\beta) \tag{7}$$

The heat transfer coefficient per unit volume, $C_{\propto\beta}^{(h)}$, in equation (7) can be obtained by:

$$C_{\alpha\beta}^{(h)} = h_{\alpha\beta} A_{\alpha\beta} \tag{8}$$

The Nusselt Number is a quantity widely used to determine the heat transfer coefficient by convection $h_{\alpha\beta}$. This inference is based on dimensional analysis, which is used to determine parameters through similarity. Thus, to find the value of $h_{\alpha\beta}$, we use:

$$Nu = 2 + 0.6Re^{0.5} Pr^{0.3} \tag{9}$$

where the Reynolds and Prandtl numbers are given as follows:

$$Pr = \frac{\mu_\alpha C_{p\alpha}}{\lambda_\alpha} \tag{10}$$

$$Re = \frac{\rho V D}{\mu} \tag{11}$$

where $C_{p\alpha}$ is the heat capacity and λ_α the thermal conductivity of the continuous phase. Them, the convective heat transfer coefficient is determinated as follows:

$$h = \frac{\lambda Nu}{d_\alpha} \tag{12}$$

The surface area per unit volume is calculated assuming that the phases are present as particles which may take various forms such as, for example, spherical defined by:

$$A_{\alpha\beta} = \frac{6f_\beta}{d_\beta} \tag{12}$$

where f_β is the volumetric fraction, d_β is the mean diameter of the particle.

3.2.2 Constitutive equations

For the core-flow, the water flows in a turbulent regime, thus, the K-ε model was chosen to calculate such effects. The equations of turbulent kinetic energy and turbulent viscous dissipation, respectively, are:

$$\frac{\partial}{\partial t}(\rho_\alpha f_\alpha K_\alpha) + \nabla \cdot \left\{ f_\alpha \left[\rho_\alpha \vec{U}_\alpha K_\alpha - \left(\mu + \frac{\mu_\alpha}{\sigma_k} \right) \nabla K_\alpha \right] \right\} = f_\alpha (G_a - \rho_\alpha \varepsilon_\alpha) \tag{14}$$

$$\begin{aligned} \frac{\partial}{\partial t}(\rho_\alpha f_\alpha K_\alpha) + \nabla \cdot \left\{ f_\alpha \rho_\alpha \vec{U}_\alpha \varepsilon_\alpha - \left(\mu + \frac{\mu_\alpha}{\sigma_\varepsilon} \right) \nabla \varepsilon_\alpha \right\} \\ = f_\alpha \frac{\varepsilon_\alpha}{K_\alpha} (C_1 G_a - C_2 \rho_\alpha \varepsilon_\alpha) \end{aligned} \tag{15}$$

where G_a a is the turbulent energy generation within the α phase, C_1 and $C_2$are empirical constants. Also in this equation, ε_α corresponds to the turbulent energy dissipation rate of the phase α and K_α the turbulent kinetic energy for the phase respectively, defined as follows:

$$\varepsilon_\alpha = \frac{C_\mu {q^3}_\alpha}{l_\alpha} \tag{16}$$

$$K_\alpha = \frac{{q^2}_\alpha}{2} \tag{17}$$

where l_α is the spatial scale length, $q_\alpha$is the velocity scale and C_μ is an empirical constant calculated by:

$$C_\mu = 4{C_\alpha}^2 \tag{18}$$

where C_α is also an empirical constant. The term μ_α corresponds to the turbulent viscosity, defined by:

$$\mu_\alpha = C_\mu \rho_\alpha \frac{{K^2}_\alpha}{\varepsilon_\alpha} \tag{19}$$

where the constants used in the previous equations are: C_1 = 1.44, C_2 = 1.99, C_μ = 0.09, σ_ε = 1.3 and σ_k = 1.0.

3.2.3 Pumping power

Some analyzes were performed based on the power required to pump the fluids involved in the flow, in order to understand aspects related to the energy efficiency of the system. To

calculate the pumping power of the system it is necessary to use a system of equations in which the power due to pressure variation, as well as the volumetric flow rate of oil and gas phases as a whole are taken into account.

Thus, the pumping power of the system P_{bs} is given by:

$$P_{bs} = \Delta P\ (Q_w + Q_O) \tag{20}$$

In a similar way, the contribution of the pumping power of both water P_{bw} and oil and gas phases P_{bo}, are given by:

$$P_{bw} = \Delta P\ x\ Q_w \tag{21}$$

$$P_{bo} = \Delta P\ x\ Q_o \tag{22}$$

3.2.4. Initial and boundary conditions

With the numerical mesh finished, a file was created to incorporate it into ANSYS CFX ® 15.1 Pre. It is possible to include the mathematical model adopted, fluid properties, type of flow regime, among others information.

With the objective of analyzing the ideal volumetric flow rates for the flow in question was simulated three-phase cases in which the pertinent considerations for the oil inlet were:

$$(R - \forall r) < r < R \Rightarrow \begin{cases} u_w = f_w = 0 \\ u_o = u_g = 1.0m/s \\ f_o = 0.95 \\ f_g = 0.05 \\ T = T_{op} \therefore 25°C \le T_{op} \le 45°C \end{cases}$$

In relation to the water inlet, was considered the following values:

$$0 < r < (R - \forall r) \Rightarrow \begin{cases} f_a = 1 \\ u_o = u_g = 0 \\ f_o = f_g = 0 \\ T = 25°C \end{cases}$$

In the outlet of the pipe was considered a pressure equal to 101.325 kPa. In the wall of the pipe we consider no-slip condition. At the begin of the process we consider that the pipe was full fill of water flowing with velocity 0.5 m/s. Table 1 shows an overview of the flow conditions for all simulated cases, where velocity (u) is given in m / s², temperature (T) in ° C, roughness (Ru) in m and volumetric fraction is dimensionless.

3.2.5 Thermal and physical properties of the fluids

Variables such as viscosity may vary greatly as the temperature changes. For example, in liquids as the temperature increases, the viscosity of the liquid is expected to decrease, whereas for the gases the reverse is the case.

Viscosity of the oil is usually defined by means of correlations. Several viscosity correlations have been proposed, but none has been used as a standard method in the petroleum industry, since the composition of crude oil is complex and often undefined. Therefore, many methods of viscosity estimation are dependent on factors such as the API degree for light, medium, heavy, ultra-heavy oils and bitumen, and they are also linked to the region where they are produced.

In this study we used the correlation reported by Sattarin et al. [18] for oil and gas, as follows:

$$\mu_o = \left(0.32 + \frac{1.8x10^7}{API^{4.53}}\right) x \left(\frac{360}{T+200}\right)^a \tag{23}$$

where the value of α is given by

$$a = antilog\left(0.43 + \frac{8.33}{oAPI}\right) \tag{24}$$

where in the API value is between 10 and 52.5.

$$\mu_w = \frac{997.2}{2.443299\,x10^{-2}x\,T - 6.153676} \tag{25}$$

The data presented in Tables 2 and 3 report all the physical characteristics assumed for the fluids in all cases studied. These properties are extremely important in understanding the physical problem, and help in interpreting the solutions.

The gas used is chemically compounded by: $CH_4 = 0.92$; $C_2H_6 = 0.055$; $C_3H_8 = 0.015$; $C_4H_{10} = 0.01$. From these values, density and viscosity of the gas phase were calculated by the Ansys CFX software. In all three-phase cases water and oil were considered as continuous phases and the gas as dispersed phase having a bubble diameter equal to 3 mm.

Table 1. Inlet data used in the simulations

Case	Oil and Gas Inlet						Water Inlet						T (°C)	Roughness (m)
	Oil		Gas		Water		Oil		Gas		Water			
	f (-)	u (m/s)	f (-)	u (m/s)	f (-)	u (m/s)	f (-)	u (m/s)	f (-)	u (m/s)	f (-)	u (m/s)		
1	0.95	1.0	0.05	1.0	0.0	0.0	0.0	0.0	0.0	0.0	1.0	0.2	25	0.0
2	0.95	1.0	0.05	1.0	0.0	0.0	0.0	0.0	0.0	0.0	1.0	0.6	25	0.0
3	0.95	1.0	0.05	1.0	0.0	0.0	0.0	0.0	0.0	0.0	1.0	1.0	25	0.0
4	0.95	1.0	0.05	1.0	0.0	0.0	0.0	0.0	0.0	0.0	1.0	1.4	25	0.0
5	0.95	1.0	0.05	1.0	0.0	0.0	0.0	0.0	0.0	0.0	1.0	1.8	25	0.0
6	0.95	1.0	0.05	1.0	0.0	0.0	0.0	0.0	0.0	0.0	1.0	2.2	25	0.0
7	0.95	1.0	0.05	1.0	0.0	0.0	0.0	0.0	0.0	0.0	1.0	2.6	25	0.0
8	0.95	1.0	0.05	1.0	0.0	0.0	0.0	0.0	0.0	0.0	1.0	3.0	25	0.0
9	0.95	1.0	0.05	1.0	0.0	0.0	0.0	0.0	0.0	0.0	1.0	3.4	25	0.0
10	0.95	1.0	0.05	1.0	0.0	0.0	0.0	0.0	0.0	0.0	1.0	3.8	25	0.0
11	0.95	1.0	0.05	1.0	0.0	0.0	0.0	0.0	0.0	0.0	1.0	5.2	25	0.0
12	0.95	1.5	0.05	1.5	0.0	0.0	0.0	0.0	0.0	0.0	1.0	0.6	45	$4.5x10^{-5}$
13	0.95	1.5	0.05	1.5	0.0	0.0	0.0	0.0	0.0	0.0	1.0	1.0	45	$4.5x10^{-5}$
14	0.95	1.5	0.05	1.5	0.0	0.0	0.0	0.0	0.0	0.0	1.0	1.4	45	$4.5x10^{-5}$
15	0.95	1.5	0.05	1.5	0.0	0.0	0.0	0.0	0.0	0.0	1.0	1.8	45	$4.5x10^{-5}$

Table 2. Thermo-physical properties of the fluids present

Physical Properties	Water	Heavy Oil	Gas
Density (kg/m³)	997	989	0.77895
Specific heat (J/kg.K)	4181.7	1700	1004.4
Thermal conductivity (W/m.K)	0.6069	0.147	0.0261

Table 3. Surface tensions between the involved phases

Water-oil	0.067 (N/m)
Water-Gas	0.07257 (N/m)
Oil-Gas	0.026 (N/m)

4. RESULTS AND DISCUSSIONS

4.1 Pressure field

Figure 4 and 5 shows the pressure profile of the three-phase flow, it can be noted that a downer region of the curvature has a greater pressure than in the upper region of the curvature. This physical situation occurs because the fluids tend to continue in the same behavior, flowing in the horizontal direction causing, which provokes an increase in pressure and the oil core is pushed to a downer part of the curvature.

4.2 Volumetric fraction field

Figure 6 and 7 illustrate the volumetric fraction fields at the instant 15s of process.

From the analysis of the Figures 6 and 7, it is possible to visualize the water film formed near the duct wall at the beginning of the flow. However, this annular pattern does not

remain stable until the end of the flow, and even almost collapses in the upper region of the curvature. In this way it is possible to affirm that in these conditions the core-flow becomes a non adequate method to be used. This is because in this region the flow is more complex due to the action of inertial, gravitational, centrifugal, and drag forces, among others. Therefore, annular flow can become a major problem, because as it is undone, the pressures become very high, causing problems in the piping.

In addition to the curved geometry of the duct, another factor that may contribute to the deconfiguration of the concentric annular profile is the presence of the gas phase, because it is less dense than other phases and tends to concentrate in the upper part of the duct, as can be seen in Figure 8.

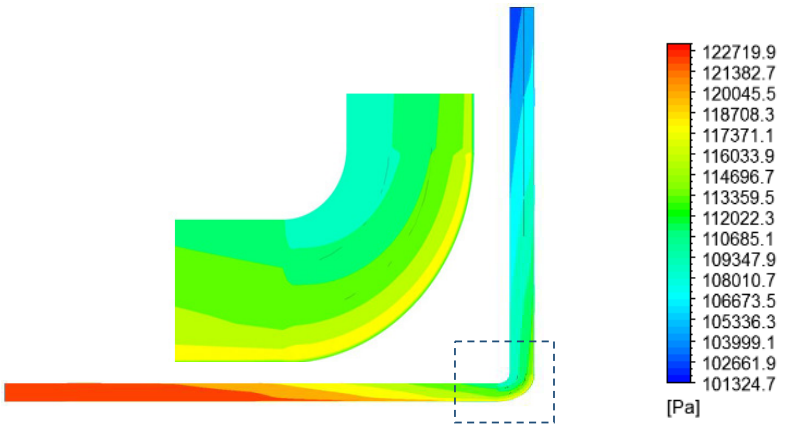

Figure 4. Pressure profile in the longitudinal plane inside the pipe at t=15 s (Case 5).

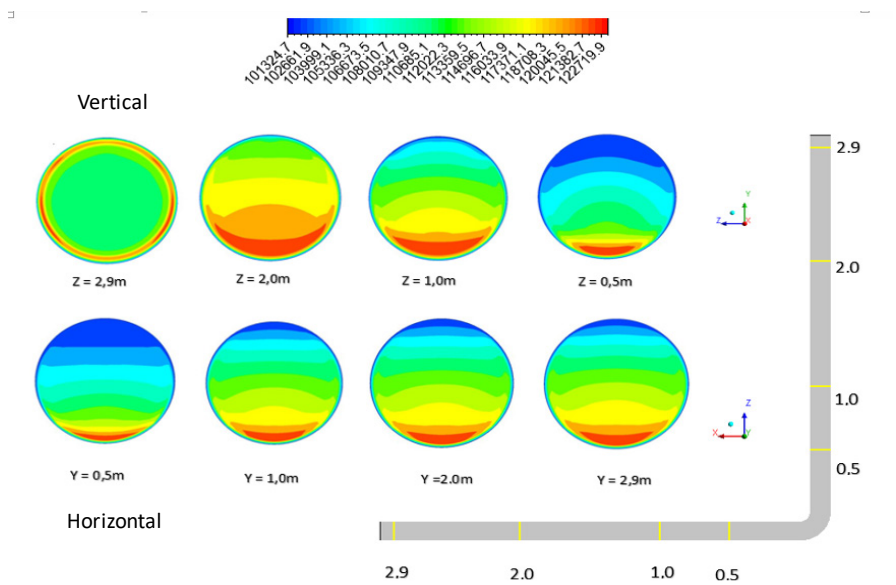

Figure 5. Pressure profile (Pa) in transverse planes inside the pipe at t =15s (Case 5)

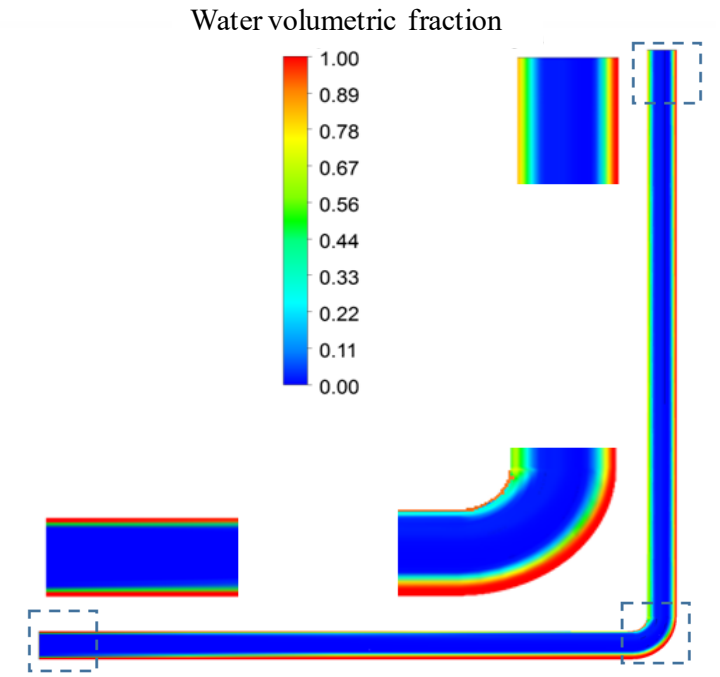

Figure 6. Volumetric fraction of water in the XY plane (Z = 0) at time t = 15 s

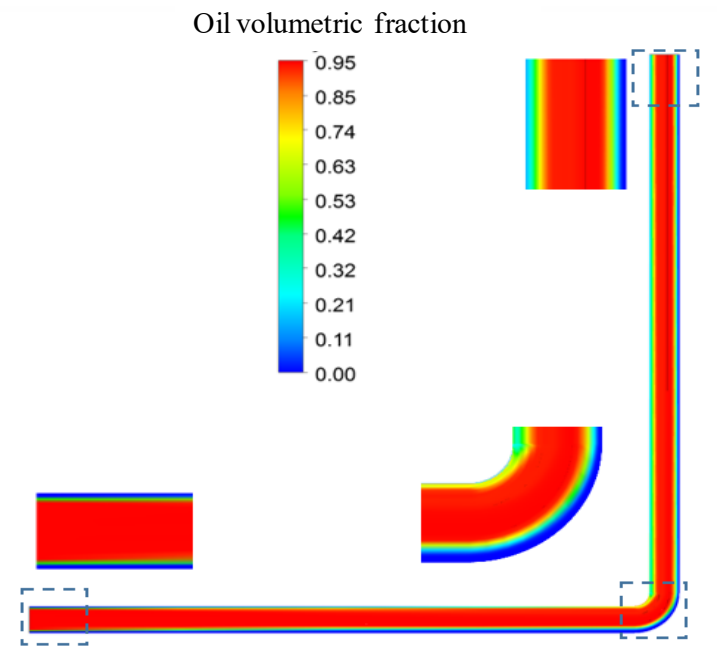

Figure 7. Volumetric fraction of oil in the XY plane (Z = 0) at time t = 15 s

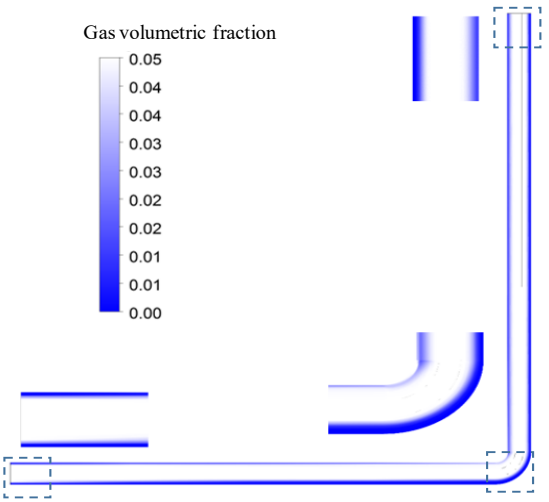

Figure 8. Volumetric fraction of gas in the XY plane (Z = 0) at t = 15s

Figure 9 shows that the water film does not remain concentric in the horizontal section near the curvature and also in the vertical straight section after the curvature. According to Bensakhria et al. [5], the radial position of the oil core in the annular flow depends solely on the ratio of the perimeter of contact between the tube wall and the fluid forming the core and the perimeter of the tube. This ratio in turn depends on the density difference between the fluids being transported and the water film as well as the amount of water injected.

Therefore, for operating with safety, a solution to this problem will be to operate with higher water flow rate, since altering the rheological properties of hydrocarbons would be a more complex task.

According to Andrade [19], an analysis of the stability of the perfect annular flow shows that this configuration is only stable for a very small set of conditions which typically do not occur in real applications but which is of interest for pipeline lubrication.

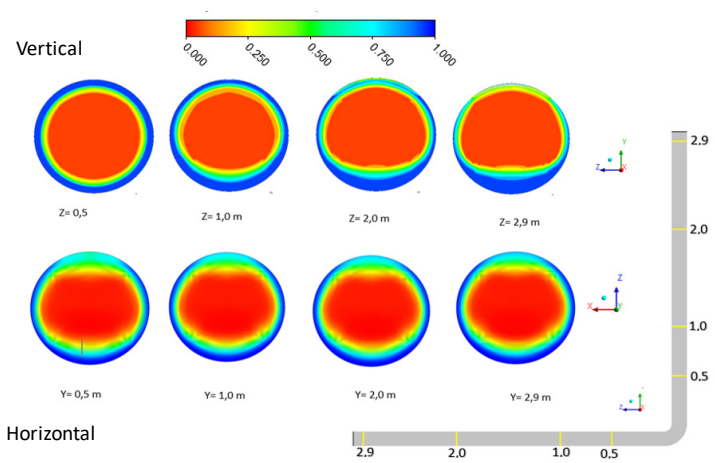

Figure 9. Volumetric fraction of the water at different transverse planes at t = 15s

4.3 Fluid transport efficiency analysis

In addition to the efficiency of the transportation guaranteed by the core-flow technique, it was also sought to achieve energy efficiency during the flow, in order to optimized ways for oil transportation. As already seen, the pumping of water, oil and gas were done at different volumetric flow rates and, therefore, with different energy consumptions.

Two sets of cases were simulated where the pumping power required to flow with different water flow rates were analyzed, setting two different oil volumetric flow rates. With these same results, both pressure drop associated to core-flow utilization and the pumping power required for such flow, were analyzed.

Table 4 presents data for the first set of simulated cases. As can be seen, the flow velocity of the oil and gas has remained constant and thus the volumetric flow rate as well. The water velocity variation occurred every 4 m / s and the pipe was considered smooth.

As both the velocity and the water flow increase, the pressure drop associated with the flow is smaller. In this way, increasing the water injection rate leads to a significant reduction in the pressure drop. The graph illustrates in Figure 10 shows this decay more clearly.

With these data, through Equations 21 to 23, it was possible to calculate the pumping power of the water, the oil and thus the power of the system. For each case studied was associated reduction of the pressure drop with the energy efficiency and finally we found the interval in which the system can operate with minimum energy necessary to guarantee the fluid flow.

Table 4. Pressure drop for different inlet velocity

Case	Water velocity (m/s)	Oil and gas velocity (m/s)	Uw/Uo	ΔP (Pa)
1	0.2	1.0	0.2	53994
2	0.6	1.0	0.6	21382
3	1. 0	1.0	1.0	14648
4	1.4	1.0	1.4	12577
5	1.8	1.0	1.8	12126
6	2.2	1.0	2.2	11466
7	2.6	1.0	2,6	10398
8	3.0	1.0	3.0	9721
9	3.4	1.0	3.4	9930
10	3.8	1.0	3.8	10560
11	5.2	1.0	5.2	12324

The graph in Figure 10 shows the range of operation in which water, oil and gas can be transported efficiently and economically; this range is between water injection velocities ranging from 0.6 m/s to 1.8 m/s.

Table 5 presents the values referring to the pumping power required for each case. By examining the pumping power of the system, it can be seen that for given water volumetric flow rate, the gains in pressure drop become constant, but the power required for fluid transportation begins to rise.

Still on the pumping power, it is observed that for the values corresponding to the oil pump there is a visible decay, clearly due to the reduction of the pressure drop. In this group of simulations, it can be stated that the ideal water injection rate should be less than 46% of the oil and gas flow rate; the water flow rate cannot exceed 0.007912458 m³/s. Thus, the best conditions for operating are around the range highlighted in Table 5.

The second group of simulations used the same physical assumptions of the previous group, changing only the oil velocity to 1.5 m/s and using a duct now with a roughness of 4.5 x 10-5 m. Higher pressure drop and consequently higher pumping power were evidently expected, both due to the higher oil flow and the influence of the roughness.

Table 5. Pumping power for different cases at t=15s

Case	Water flow rate (m³/s)	Oil and gas flow rate (m³/s)	Water pumping power (W)	Oil and gas pumping power (W)	Pumping Power System (W)
1	0.000879176	0.0132661	47.47	716.28	763.76
2	0.002637528	0.0132661	56.39	475.43	538.44*
3	0.004395880	0.0132661	64.39	194.32	340.05*
4	0.006154232	0.0132661	77.40	166.84	277.15*
5	0.007912584	0.0132661	87.46	164.96	258.71*
6	0.009670936	0.0132661	103.70	156.48	260.19
7	0.011429288	0.0132661	116.89	146.98	263.88
8	0.013187640	0.0132661	125.49	135.26	266.75
9	0.014945992	0.0132661	128.19	128.95	270.87
10	0.016704344	0.0132661	157.14	151.73	288.05

*Operating range

In order to understand the behavior of the fluids under the effect of a higher temperature, four cases were run in which we tried to analyze what will be the best operating range for these configurations. Table 6 shows the values adopted for the flow.

Table 6. Pressure drop for different inlet velocity of water (t=15 s)

Case Study	Water velocity (m/s)	Oil and gas velocity (m/s)	Uw/Uo	ΔP (Pa)	
				T= 45 °C	T= 25 °C
Case 12	0.6	1.5	0.40	30818	51217
Case 13	1.0	1.5	0.66	21799	22004
Case 14	1.4	1.5	0.93	15019	14997
Case 15	1.8	1.5	1.20	12507	12499

As the temperature increases, it is observed that the oil viscosity decreases, a fact which consequently facilitates the transport of heavy oil. Thus, when analyzing Figure 11, it can be seen that for low Uw/Uo ratios the pressure differential is around 31000 Pa, a lower value as compared with the cases where lower temperatures is used.

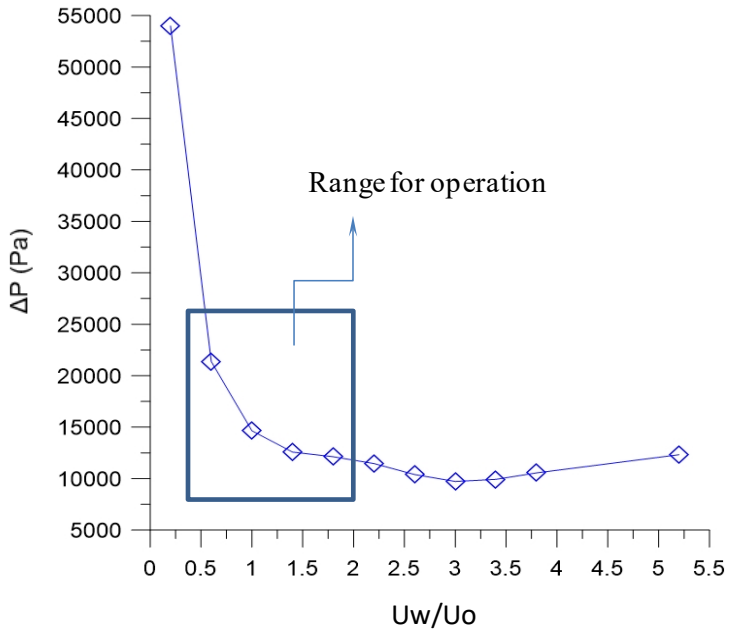

Figure 10. Pressure drop as a function of the water velocity

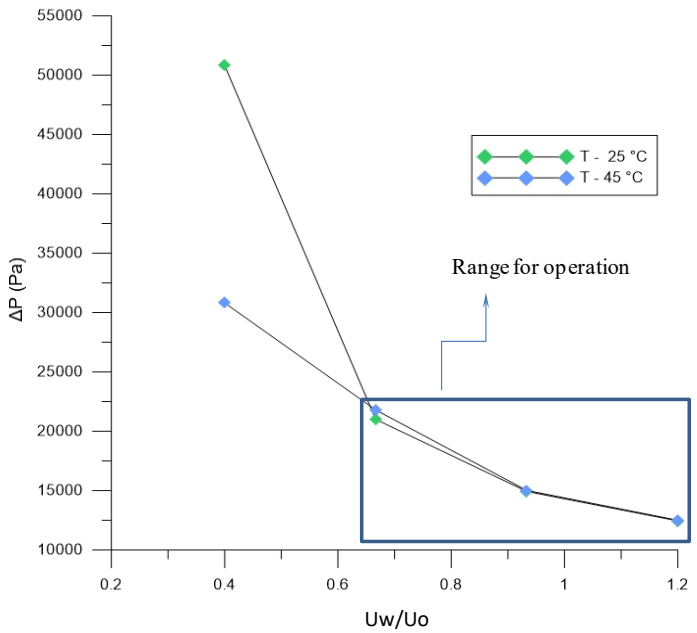

Figure 11. Pressure drop as a function of water velocity at t=15s

The increase in temperature also influences the operating range, as the pressure drop becomes constant more rapidly, so the operating range is reached with lower water flow rate, as can be seen in Table 7.

Table 7. Pumping power for different cases at t=15s (T= 45 °C)

Case	Water flow rate (m^3/s)	Oil and gas flow rate (m^3/s)	Water pumping power (W)	Oil and gas pumping power (W)	Pumping Power System (W)
12	0.002637528	0.01989915	81.28	613.25	694.53
13	0.00439588	0.01989915	95.82	433.78	529.60*
14	0.006154232	0.01989915	92.43	298.86	391.29*
15	0.007912584	0.01989915	98.96	248.87	347.84*

5. CONCLUSIONS

Considering the simulations of oil and water single-phase flows, and heavy oil, water and gas three-phase flows, in curved ducts we can concluded that:

a) There is a significant reduction in the pressure drop along the flow for the three-phase cases proving the efficiency of the transport of heavy oils using the core-flow technique;
b) The maintenance of the water film along the flow becomes sensitive in regions where the geometry becomes complex allowing adverse situations such as variations of the velocity field and recirculation zones as in pipe with curvature.
c) The ideal water volumetric flow rate must not be too much low or very high, because in the first case it does not form the annular profile, making the desired reduction of the pressure drop impossible. In the second, excessive volumetric flow rates can generate unnecessary energy consumption and even affect the stability of the annular profile.
d) The presence of the gas directly influences the formation of the water film on the inner wall of the duct. Because it is a less dense fluid, it tends to concentrate in the upper parts of the duct, causing a greater misconfiguration of the water film in the upper region.
e) There is an optimized operating range in terms of pumping power. This is directly related to the maximum capacity required for water injection.
f) The increase in temperature reduces pressure drop and consequently provokes changes in the operating range. Thus, it can be reached with lower water volumetric flow rate.

ACKNOWLEDGMENT

The authors thanks to ANP/UFCG/PRH-42, CAPES, CNPq and FINEP (Brazilian Research Agencies) and PETROBRAS (Brazilian Oil Company), for all financial support and the researchers cited in the text which help in improvement.

REFERENCES

[1] Trevisan, F. E. Flow Patterns and Pressure Drop in Horizontal Three-Phase Flow of Heavy Oil, Water and Air, Petroleum Sciences and Engineering, Faculty of Mechanical Engineering, State University of Campinas (UNICAMP), 2003. (In Portuguese)

[2] Silva, R.C.R. Variations in Wettability of Internal Surfaces of Pipes Used in the Transport of Heavy Oils Via Core-flow. Master's Dissertation Petroleum Sciences and Engineering, Faculty of Mechanical Engineering, State University of Campinas (UNICAMP), Campinas, Brazil, 2003. (In Portuguese).

[3] Russel, T.W.F.; Hodgson, G.W.; Govier, G.W. (1959) Horizontal Pipeline Flow of Mixtures of Oil and Water, Canadian Journal of Chemical Engineering. 37(1), p. 9-17.

[4] Obregón, V.; Rosa, M. Hydrodynamics of the Heavy Oil-Water Two-phase Flow in Horizontal Tube. Master´s Dissertation, Mechanical Engineering, State University of Campinas, (UNICAMP), Campinas, Brazil, 2000. (In Portuguese)

[5] Bensakhria, A.; Peysson, Y.; Antonini, G. (2004) Experimental Study of the Pipeline Lubrication for Heavy Oil Transport. Oil & Gas Science and Technology, 59(5), p.523-533.

[6] Ghosh, S.; Mandal, T. K.; Das, G.; Das, P. K. (2009) Review of Oil Water Core Annular Flow. Renewable and Sustainable Energy Reviews, 13(8), p.1957 – 1965.

[7] Wegmann, A.; Melke, J.; Rohr, P. R. (2007) Three-phase Liquid–Liquid–Gas Flows in 5.6 mm and 7 mm Inner Diameter Pipes. International Journal of Multiphase Flow, 33(5), p.484-497.

[8] Poesio, P.; Sotgia, G.; Strazza, D. (2009)Experimental Investigation of Three-Phase Oil-Water-Air Flow Through a Pipeline. Multiphase Science and Technology, 21(1-2), p. 107-122.

[9] Wang, L.-Y.; Wu, Y.-X.; Zheng, Z.-C.; Guo, J.; Zhang, J.; Tang, C. (2008) OilWater Two-Phase Flow Inside T-Junction. Journal of Hydrodynamics, 20(2), p. 147-153.

[10] Andrade, T. H. F.; Silva, F. N.; Farias Neto, S. R.; Lima, A. G. B. (2013) Applying CFD in the Analysis of Heavy oil - Water Two-phase Flow in Joints by Using Core Annular Flow Technique. The International Journal of Multiphysics, 7, p.137 - 152.

[11] Andrade, T. H. F.; Silva, F. N.; Farias Neto, S. R.; Lima, A. G. B.; SILVA, C. J.; Lima, W. M. P. B.(2014) Operation Control of Fluids Pumping in Curved Pipes During Annular Flow: A Numerical Evaluation. The International Journal of Multiphysics. 8, p.271-284.

[12] Andrade, T. H. F.; Crivelaro, K. C. O.; Farias Neto, S. R.; Lima, A. G. B. (2013) Isothermal and Non-isothermal Water and Oil Two-phase Flow (Core-flow) in Curved Pipes. The International Journal of Multiphysics. 7, p.167-182.

[13] Andrade, T. H. F., Crivelaro, K. C. O., Farias Neto, S. R.; Lima, A. G. B. Numerical Study of Heavy Oil Flow on Horizontal Pipe Lubricated by Water. In: Materials with Complex Behaviour II: Properties, Non-Classical Materials and New Technologies. Series: Advanced Structured Materials.1 ed. Heidelberg (Germany): Springer-Verlag, 2012, v.16, p. 99-118.

[14] Crivelaro, K. C. O.; Damacena, Y. T.; Andrade, T. H. F.; Lima, A. G. B.; Farias Neto, S. R. (2009) Numerical Simulation of Heavy Oil Flows in Pipes Using The Core-Annular Flow Technique. WIT Transactions on Engineering Sciences (Online). 63, p.193 - 203.

[15] Brauner, N. (1991) Two-Phase Liquid-Liquid Annular Flow, International Journal of Multiphase Flow, 17(1), p. 59-76.

[16] Vanegas, P. J. W. Experimental Study of the Core-Flow in Ultra-viscous Oils Elevation - (Master´s Dissertation), Faculty of Mechanical Engineering, State University of Campinas, Campian, Brazil, 1998. (In Portuguese).

[17] Bannwart, A. C. (2001) Modeling Aspects of Oil-Water Core-annular-flows. Journal of Petroleum Science and Engineering, 32(2), p.127-143.

[18] Sattarin, M.; Modarresi, H.; Bayat, M.; Teymori, M. (2007) New viscosity correlations for dead crude oils. Petroleum & Coal. 49(2), p. 33-39.

[19] Andrade, T. H. F. Ultra-viscous Heavy-oil Transportation via Core-Flow: Geometrical e Thermo Fluid Dynamic Aspects. PhD Thesis (Process Engineering), Federal University of Campina Grande, Campina Grande, Brazil, 2013. (In Portuguese)